U-spin-*CP* anomaly in charm

Rigo Bause,[1,*] Hector Gisbert,[1,†] Gudrun Hiller,[1,‡] Tim Höhne,[1,§] Daniel F. Litim,[2,‖] and Tom Steudtner[1,¶]
[1]*Department of Physics, TU Dortmund University, Otto-Hahn-Strasse 4, D-44221 Dortmund, Germany*
[2]*Department of Physics and Astronomy, University of Sussex, Brighton, BN1 9QH, United Kingdom*

(Received 10 November 2022; accepted 11 July 2023; published 1 August 2023)

The recent measurement of the *CP* asymmetry in the decay $D \to K^+K^-$ by LHCb, combined with ΔA_{CP}, evidences a sizable *CP* asymmetry in the decay $D \to \pi^+\pi^-$, which requires a dynamical enhancement of standard model higher-order contributions over tree-level ones by a factor of 2. The data furthermore imply huge *U*-spin breaking, about 4–5 times larger than the nominal standard model one of $\lesssim 30\%$ in charm. Enhanced breakdown of the two approximate symmetries points to models that violate *U*-spin and *CP* and disfavors flavor singlet contributions such as chromomagnetic dipole operators as explanations of the data. We analyze the reach of flavorful Z' models for charm *CP* asymmetries. Models generically feature explicit *U*-spin and isospin breaking, allowing for correlations with $D \to \pi^0\pi^0$ and $D^+ \to \pi^+\pi^0$ decays with corresponding *CP* asymmetries at similar level and sign as $D \to \pi^+\pi^-$, about $\mathcal{O}(1-2) \times 10^{-3}$. Experimental and theoretical constraints very much narrow down the shape of viable models: Viable, anomaly-free models are leptophobic—or at least electron- and muophobic—with light Z' below $\mathcal{O}(20)$ GeV and can be searched for in low mass dijets at the LHC or in Υ and charmonium decays, as well as dark photon searches. A Z' around ~ 3 or $\sim(5\text{–}7)$ GeV can relieve the tensions in the $J/\psi \to \pi^+\pi^-$ and $\psi' \to \pi^+\pi^-$ branching ratios with pion form factor values from fits to *BABAR* and JLab data and simultaneously explain the charm *CP* asymmetries. Models can also feature sizable branching ratios into light right-handed neutrinos or vectorlike dark fermions, which can be searched for in $e^+e^- \to$ hadrons + invisibles at Belle II and BESIII. Because of the low new physics scale, dark fermions can easily induce an early Landau pole, requiring models to be UV completed near the TeV scale.

DOI: 10.1103/PhysRevD.108.035005

I. INTRODUCTION

The LHCb Collaboration measured the *CP* asymmetry in $D^0 \to K^+K^-$ decays [1],

$$A_{CP}(K^+K^-) = (6.8 \pm 5.4 \pm 1.6) \times 10^{-4}, \tag{1}$$

where the first and second errors are statistical and systematic, respectively. Together with the previous LHCb measurement [2]

$$\begin{aligned}\Delta A_{CP} &= A_{CP}(K^+K^-) - A_{CP}(\pi^+\pi^-) \\ &= (-15.4 \pm 2.9) \times 10^{-4},\end{aligned} \tag{2}$$

LHCb performed a fit determining both direct *CP* asymmetries [1],

$$\begin{aligned}a^d_{K^-K^+} &= (7.7 \pm 5.7) \times 10^{-4}, \\ a^d_{\pi^-\pi^+} &= (23.2 \pm 6.1) \times 10^{-4},\end{aligned} \tag{3}$$

with a correlation $\rho(a^d_{K^-K^+}, a^d_{\pi^-\pi^+}) = 0.88$ and leading to 3.8σ evidence of *CP* violation in $D^0 \to \pi^+\pi^-$ decays. This is puzzling for two reasons: First, the *CP* asymmetry $a^d_{\pi^-\pi^+}$ is larger than $|\Delta A_{CP}|$. Therefore, a standard model (SM) interpretation of the former needs even more dynamical enhancement of higher-order contributions h over the tree-level amplitude t to compensate the Cabibbo-Kobayashi-Maskawa (CKM) suppression $a^{d\mathrm{SM}}_{\pi^-\pi^+} \sim 2 \cdot \mathrm{Im}(V^*_{cb}V_{ub}/(V^*_{cd}V_{ud}))h/t \sim 1.2 \times 10^{-3} h/t$, with data (3) pointing to $h/t \sim 2$. Here an order one strong phase is assumed, and the enhancement is even bigger if the latter is suppressed, see Appendix A for details. Second, the new result implies

*rigo.bause@tu-dortmund.de
†hector.gisbert@tu-dortmund.de
‡ghiller@physik.uni-dortmund.de
§tim.hoehne@tu-dortmund.de
‖d.litim@sussex.ac.uk
¶tom2.steudtner@tu-dortmund.de

a violation of U-spin symmetry, that is, violation of $a^d_{K^-K^+} = -a^d_{\pi^-\pi^+}$, at the level of 2.7σ [1]. Two approximate symmetries of the SM are thus being challenged. While it is too early to draw firm conclusions given the significant hadronic uncertainties in D decays, the recent data make new physics (NP) searches with rare charm decays just more interesting—this could be a hint for flavorful physics beyond the SM.

This interplay of the CP asymmetries is illustrated in Fig. 1. The small value of $A_{CP}(K^+K^-)$, combined with ΔA_{CP} (green-shaded area), implies a sizable CP asymmetry in $\pi^+\pi^-$, together with substantial U-spin breaking, which has also been pointed out in [3]. Predictions in the U-spin limit (red dashed line) and $\lesssim$30% SM-like breaking (red-shaded cones) are indicated. The LHCb fit (orange-shaded area) is two sigmas outside of this cone. The U-spin splitting in the $D \to \pi^+\pi^-$ and $D \to K^+K^-$ branching ratios is very well known [4] and can be explained within the SM with $\lesssim$30% breaking, for instance, [5–7]. Roughly speaking, because $\frac{(1+1/3)^2}{(1-1/3)^2} = 4$ an assumed 33% contribution to both decays of opposite sign is more than enough to explain the enhancement of $\mathcal{B}(D \to K^+K^-)/\mathcal{B}(D \to \pi^+\pi^-) \simeq 2.8$, with or without considering the different phase space or factorizable flavor breaking from, e.g., decay constants and form factors [8]. The splitting in the leading SM decay amplitudes suggests a modified U-spin relation, see Appendix A,

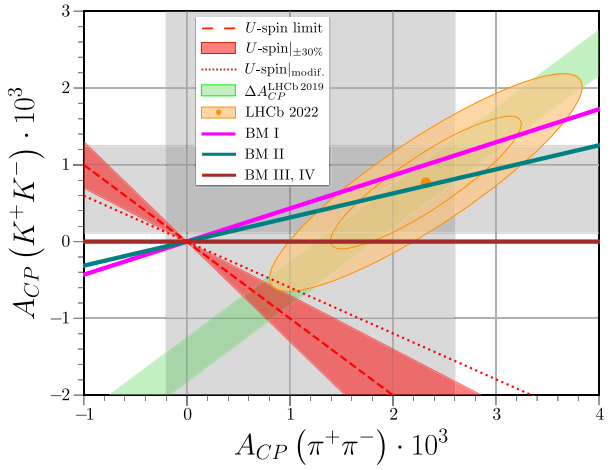

FIG. 1. The U-spin-CP anomaly in charm, showing bounds (2) from LHCb on ΔA_{CP} (green-shaded area), bounds from (3) on $A_C P(K^+K^-)$, and $A_C P(\pi^+\pi^-) = (12 \pm 14) \times 10^{-4}$ from the Heavy Flavor Averaging Group (HFLAV) [9] (gray-shaded areas). Values of $a^d_{K^-K^+}$ and $a^d_{\pi^-\pi^+}$ from (3) are shown with correlation at 68% and 95% CL [1] (orange-shaded). Also shown is the U-spin limit (red dashed line) together with $\lesssim$30% SM-like breaking (red cones), and the modified U-spin relation (4) (red dotted line). Thick straight lines relate to the new benchmark models of this work: BM I (magenta), BM II (teal), BM III (for $G = 0$), and BM IV (both brown), see Table I.

$$\frac{a^d_{K^-K^+}}{a^d_{\pi^-\pi^+}} = -\sqrt{\frac{\mathcal{B}(D \to \pi^+\pi^-)}{\mathcal{B}(D \to K^+K^-)}}, \tag{4}$$

also indicated in Fig. 1 (dotted red line). Even though this effect slightly alleviates the anomaly, it still leaves the bulk of it unaltered, and the quest for models to explain it remains open.

Enhanced chromomagnetic dipole operators such as from supersymmetric loops are flavor singlets, feature therefore SM-like symmetries, and are not able to account for the significant U-spin breaking. Models that generically break flavor beyond the SM are Z' models with generation-dependent charges. Their impact on CP asymmetries in charm has been studied in [10].

In this work, we analyze the new data (3) within flavorful $U(1)'$ extensions of the SM. Interestingly, due to empirical constraints it turns out that the Z' mass has to be below the weak scale to induce a per-mill level CP asymmetry in charm. This is an important finding and we plan to derive it step by step in the paper: Z' models and constraints from charm processes are discussed in Sec. II, pointing to a low mass Z' of $\mathcal{O}(10)$ GeV. In Sec. III, we work out constraints applicable to this mass range from searches in dilepton and dijet signatures and quarkonium decays. In Sec. IV, we analyze the high energy behavior, including Landau poles. In Sec. V, we conclude. SM decay amplitudes and observables are parametrized in Appendix A. Details on the estimation of hadronic parameters are given in Appendix B. Charges for leptophobic, anomaly-free models with vanishing one-loop kinetic mixing are derived in Appendix C, and their higher-order kinetic mixing is studied in Appendix D.

II. FLAVORFUL Z' MODELS

We consider the SM extended by an Abelian gauge group, with generation-dependent charges to fundamental fermions. We present the model setup in Sec. II A and work out constraints from charm in Sec. II B. In Sec. II C, predictions for CP asymmetries in $D \to \pi^0\pi^0$ and $D^+ \to \pi^+\pi^0$ are given.

A. Z' model setup

We denote the $U(1)'$ charges of the SM fermions $\psi = Q$, U, D, L, E and possibly also right-handed neutrinos ν_R as F_{ψ_i}, where $i = 1, 2, 3$ corresponds to the generation label. The charges are subject to anomaly cancellation conditions (C1)–(C6). The SM Higgs is uncharged under the $U(1)'$ to avoid mixing with the electroweak sector. The theory has a rescaling invariance with a constant k as $F_\psi \to kF_\psi$, $g_4 \to g_4/k$, where g_4 denotes the $U(1)'$-gauge coupling. It is therefore useful to consider rescaling invariant quantities such as $F_\psi g_4$, $F_\psi/F_{\psi'}$, or $\mathrm{d}g_4/g_4$. Here we choose to show integer charges for notational convenience.

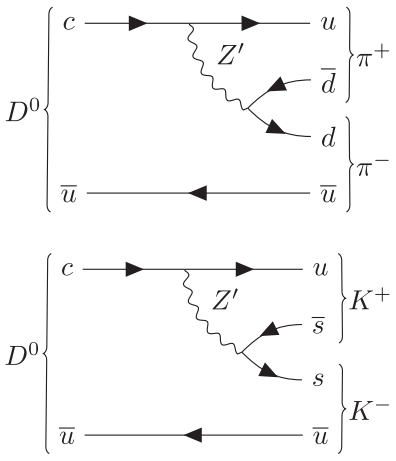

FIG. 2. Contributions of the Z' boson to $D^0 \to \pi^+\pi^-$ (top diagram) and $D^0 \to K^+K^-$ (bottom diagram) amplitudes.

The Z' induces $D^0 \to \pi^+\pi^-$ and $D^0 \to K^+K^-$ at tree level, as illustrated in Fig. 2. Contributions to the CP asymmetries in (3) can be parametrized as [10][1]

$$a^d_{K^-K^+} = \frac{g_4^2}{M_{Z'}^2}\Delta\tilde{F}_R[c_K F_{Q_2} + d_K F_{d_2}],$$
$$a^d_{\pi^-\pi^+} = \frac{g_4^2}{M_{Z'}^2}\Delta\tilde{F}_R[c_\pi F_{Q_1} + d_\pi F_{d_1}], \tag{5}$$

where $c_{\pi,K}, d_{\pi,K}$ are hadronic parameters (see Appendix B) and

$$\Delta\tilde{F}_R = \sin\theta_u \cos\theta_u (F_{u_2} - F_{u_1}) \tag{6}$$

stands for the right-handed $c \to u$ flavor-changing neutral current (FCNC) coupling. As apparent, it requires nonuniversal charges $F_{u_2} \neq F_{u_1}$, as well as mixing between first and second generation right-handed up quarks, described by the angle θ_u. We treat θ_u as a free parameter and adjust it accordingly. We assume that the corresponding angle in the down sector is sufficiently small to avoid kaon constraints. For the same reason, we consider only models with $F_{Q_{1,2}} = 0$.[2] Explaining a sizable $a^d_{\pi^-\pi^+}$ and near or even SM-like $a^d_{K^-K^+}$ poses a challenge to beyond the standard model (BSM) building. To estimate the maximal reach, we assumed in (5), which arises from interference between the SM and the Z' amplitudes, that the relative strong and CP phases are maximal. Having the latter near $\pi/2$ also evades constraints from CP violation in D mixing, see [10] for details.

The efficiency of the BSM model in explaining data (3) is determined by the hadronic parameters $d_{K,\pi}, c_{K,\pi}$ [10], of which here only d_π, d_K matter. They include the leading-order renormalization group (RG) running of Wilson coefficients in the weak effective theory from $M_{Z'}$ to the charm mass scale, as well as the hadronic matrix elements. The latter are subject to sizable hadronic uncertainties [10–13], see Appendix B for details. The resulting CP asymmetries serve rather as an indication of what is achievable in Z' models.

To construct models, that is, identify suitable charge assignments, which account for the new LHCb results on CP violation in charm (3), we follow similar lines as [10]: Our starting point is the cancellation of gauge anomalies, decoupling from kaons $F_{Q_{1,2}} = 0$, inducing an $c \to u$ FCNC $F_{u_2} \neq F_{u_1}$ and explicit U-spin breaking $F_{d_2} \neq F_{d_1}$. Absence of one-loop-induced $Z - Z'$ mixing is preferred. In the following, the models are further narrowed down. We discuss the theoretical and experimental constraints that arise and the corresponding selection criteria for charge patterns, which lead to the benchmark models, Table I.

Let us also ask about the mass scale one would generically expect to address (3) from Z'-tree-level exchange. Very roughly, assuming order one couplings, $g_4^2\Delta\tilde{F}_R F_{d_1} \sim 1$, this gives a Z' mass around

$$M_{Z'} \sim (3\sqrt{2}G_F V^*_{cd} V_{ud} a^d_{\pi^-\pi^+})^{-1/2} \sim 7\ \text{TeV}, \tag{7}$$

where RG effects in d_π reduce this to the few TeV range, see (5), Appendix B, and [10] for details. In the next section, we learn that the constraints from D mixing require suppressed couplings and a significantly lighter Z' than (7).

B. Charming constraints

We discuss constraints from charm CP asymmetries, D-meson mixing, $D^0 \to \mu^+\mu^-$, and on $\bar{u}c + \bar{c}u \to \ell^+\ell^-$, $\ell = e, \mu, \tau$ from Dell-Yan production, as well as charm to invisibles.

1. Charm CP asymmetries

Using Eqs. (3) and (5) with $F_{Q_{1,2}} = 0$, the ratio between F_{d_2} and F_{d_1} is fixed,

$$\frac{F_{d_2}}{F_{d_1}} = \frac{d_\pi a^d_{K^-K^+}}{d_K a^d_{\pi^-\pi^+}} \simeq -0.42^{+0.83}_{-0.13}, \tag{8}$$

resulting in a large hierarchy $|F_{d_2}| \ll |F_{d_1}|$. The uncertainty in Eq. (8) is computed from the χ^2 function

[1]The Z' induces also annihilation-type contributions to the $D^0 \to \pi^+\pi^-$ and $D^0 \to K^+K^-$ amplitudes. Annihilation contributions are power suppressed and require gluon exchange; however, the actual size of suppressions in D decays is within wider ranges [11]. We, therefore, refrain from including them in the numerical analysis, as we are focusing on the reach of models addressing data (3). In addition, note that contributions induced by F_{u_1} do not break U-spin.

[2]This is also the reason why we do not consider scalar singlet mediators contributing predominantly to $D^0 \to \pi^+\pi^-$ decays: They would couple to left-handed (and right-handed) down quarks, and after CKM mixing induce $\bar{d}s$-FCNCs, which are severely constrained.

TABLE I. Benchmarks for anomaly-free $U(1)'$—extensions of the SM + $3\nu_R$. BM I, II, and IV avoid $Z - Z'$ mixing at one loop, while BM III does not. Note, $|G/F| \ll 1$ due to (8), and $G = 0$ is also possible. BM IV may or may not contain right-handed neutrinos, in which case $F_\nu = 0$. It also can feature integer charges with hierarchy $|F_e| \ll |F_u|, |F_d|$, in which case it becomes leptophobic, see Appendix C for details and construction. Because of sizable couplings to electrons or muons, the BMs I and II are excluded (34) by $Z' \to ee, \mu\mu$ searches for a light Z'. While, in general, the ordering of generations is arbitrary due to permutation invariance, we use the ordering as stated here (the ith entry corresponds to the ith generation). Note, BM III with only the charges in the right-handed up sector swapped, $F_{u_1} = -F, F_{u_2} = G$, is equally viable; we refer to it as BM III-s.

Model	F_{Q_i}			F_{u_i}			F_{d_i}			F_{L_i}			F_{e_i}			F_{ν_i}		
BM I	0	0	0	9	−16	7	20	−11	−9	15	−6	−9	−16	0	16	6	12	−18
BM II	0	0	0	−19	9	10	20	−8	−12	4	1	−5	15	2	−17	8	2	−10
BM III	0	0	0	G	$-F$	0	F	$-G$	0	0	0	0	0	$-G$	F	0	G	$-F$
BM IV	0	0	0	$-F_u$	F_u	0	F_d	0	$-F_d$	0	0	0	F_e	0	$-F_e$	F_ν	$-F_\nu$	0

$\chi^2(a^d_{\pi^-\pi^+}, a^d_{K^-K^+})$ with correlations included. This function can be expressed in terms of $a^d_{\pi^-\pi^+}$ (or $a^d_{K^-K^+}$) and the ratio $a^d_{K^-K^+}/a^d_{\pi^-\pi^+}$. We extract the uncertainty imposing $\Delta\chi^2 = 1$ and scanning $a^d_{\pi^-\pi^+}$ (or $a^d_{K^-K^+}$) within its 1σ range. The nonparabolic behavior results in asymmetric uncertainties. Similar results were obtained in Ref. [3].

Note that renormalization group equation (RGE) effects cancel in the ratio $d_\pi/d_K = -a_K/a_\pi \simeq -1.27 \pm 0.10$ [10], therefore Eq. (8) is independent of the Z' mass, and only a parametric dependence with the quantities $a_{\pi,K}$ extracted from measured $D^0 \to \pi^+\pi^-$ and $D^0 \to K^+K^-$ branching ratios survive [10]. Given the order of magnitude of $a^d_{K^-K^+}$, within the ballpark of SM estimations, we also consider models with $F_{d_2} = 0$.

2. D-meson mixing

D-meson mixing constrains right-handed up-quark couplings as

$$\frac{g_4 \Delta\tilde{F}_R}{M_{Z'}} < 7.1 \times 10^{-4}\ \text{TeV}^{-1} (95\%\,\text{C.L.}), \tag{9}$$

where the right-hand side of this equation depends mildly on the Z' mass from RGE effects (it is a few percent for $M_{Z'} \in [10, 10^4]$ GeV.) The limit (9) takes into account the recent update from HFLAV Collaboration [9] where the new D-mixing experimental data from LHCb have been included [14]. The bound for heavy Z' masses is somewhat stronger than the previous one, 8×10^{-4} TeV^{-1} [10].

The available parameter space is presented in Fig. 3 in a way that is independent of the $U(1)'$ charge normalization. Shown are curves in $g_4 F_{d_1}/M_{Z'}$ versus $\Delta\tilde{F}_R/F_{d_1}$ that explain $a^d_{\pi^-\pi^+}$, with uncertainties from data (3) which have been increased with an additional 30% of uncertainty to account for hadronic effects. Roughly,

$$g_4 F_{d_1}/M_{Z'} \sqrt{\Delta\tilde{F}_R/F_{d_1}} \sim 0.16\ \text{TeV}^{-1}. \tag{10}$$

In addition, the excluded 95% C.L. region by D mixing (9) is shown in red. Thus, $\Delta\tilde{F}_R/F_{d_1} \ll 1$ via small mixing θ_u is instrumental to generate sizable CP asymmetries while simultaneously avoiding D-mixing constraints. We recall that $\Delta\tilde{F}_R$ (6) contains the mixing angle θ_u which can be freely adjusted. We provide other (central) values of $a^d_{\pi^-\pi^+}$ as black dashed lines. We learn that the minimal value of $g_4 F_{d_1}/M_{Z'}$ with current data is around $\sim$30 TeV^{-1}, suggesting a low, subelectroweak Z' mass.

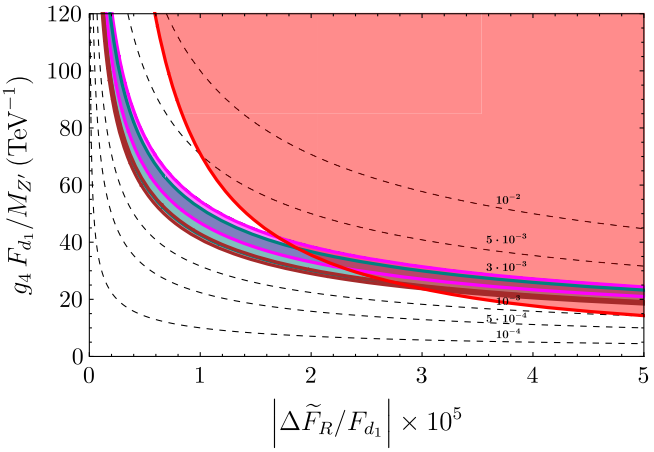

FIG. 3. $g_4 F_{d_1}/M_{Z'}$ as a function of $\Delta\tilde{F}_R/F_{d_1}$ and $d_\pi \simeq 0.1$ TeV^2. The red area represents the excluded 95% C.L. region by D mixing (9). The parameter space of models BM I, II, and III (with $G = 0$) from Table I accounting for the experimental results of ΔA_{CP} and $a^d_{\pi^-\pi^+}$ within its 1σ range are shown in magenta, teal, and brown, respectively. BM IV has the same parameter space as BM III (with $G = 0$). The shaded bands include an additional 30% of hadronic uncertainty. The semianalytical expressions of these regions are $g_4 F_{d_1}/M_{Z'} = c(\Delta\tilde{F}_R/F_{d_1})^{-1/2}$ with factor $c = 0.160 \pm 0.012$ TeV^{-1} (magenta), 0.149 ± 0.015 TeV^{-1} (teal), and 0.133 ± 0.003 TeV^{-1} (brown). The black dashed lines illustrate different values of $a^d_{\pi^-\pi^+}$.

3. Charm dilepton and invisibles data

Concerning charming dilepton processes, the constraints from branching ratios of (semi)muonic D decays read [15,16]

$$g_4^2|\Delta\tilde{F}_R|\sqrt{F_{L_2}^2+F_{e_2}^2}\lesssim 0.02\left(\frac{M_{Z'}}{\text{TeV}}\right)^2, \tag{11}$$

$$g_4^2|\Delta\tilde{F}_R(F_{L_2}-F_{e_2})|\lesssim 0.02\left(\frac{M_{Z'}}{\text{TeV}}\right)^2. \tag{12}$$

Here, we employed the recent LHCb measurement [15],

$$\mathcal{B}(D^0\to\mu^+\mu^-)<2.9\times10^{-9}(90\%\,\text{C.L.}), \tag{13}$$

which is a factor 2 stronger than the previous one. For $\ell=e,\tau$ Drell-Yan constraints [17] are stronger than those from rare decays,

$$g_4^2|\Delta\tilde{F}_R|\sqrt{F_{L_1}^2+F_{e_1}^2}\lesssim 0.06\left(\frac{M_{Z'}}{\text{TeV}}\right)^2, \tag{14}$$

$$g_4^2|\Delta\tilde{F}_R|\sqrt{F_{L_3}^2+F_{e_3}^2}\lesssim 0.12\left(\frac{M_{Z'}}{\text{TeV}}\right)^2. \tag{15}$$

Using the relation (10) imposed by $a^d_{\pi^-\pi^+}$, displayed in Fig. 3, the dilepton bounds are satisfied if

$$|F_{L_2}-F_{e_2}|,\sqrt{F_{L_2}^2+F_{e_2}^2}\lesssim 0.8|F_{d_1}|, \tag{16}$$

$$\sqrt{F_{L_1}^2+F_{e_1}^2}\lesssim 2.3|F_{d_1}|, \tag{17}$$

$$\sqrt{F_{L_3}^2+F_{e_3}^2}\lesssim 4.7|F_{d_1}|, \tag{18}$$

that is, couplings to the leptons should not be excessive compared to the ones to the quarks.

We also work out limits from data on $c\to u$ plus missing energy. Missing energy can stem from right-handed neutrinos ν and/or vectorlike dark BSM fermions χ charged under the $U(1)'$ only, with mass not exceeding $m_D/2\approx 0.9$ GeV. We start with $D^0\to\pi^0+$ invisibles, whose branching ratio is constrained by BESIII data [18]

$$\mathcal{B}(D^0\to\pi^0\ \text{inv.})<2.1\times10^{-4}(90\%\,\text{C.L.}). \tag{19}$$

Neglecting finite m_χ corrections, the branching ratio can be written as [19,20]

$$\mathcal{B}(D^0\to\pi^0\nu\bar{\nu},\chi\bar{\chi})\approx\frac{2\pi^2A_+}{G_F^2\alpha_e^2}\left(\frac{g_4^2\Delta\tilde{F}_RF_{\nu,\chi}}{M_{Z'}^2}\right)^2, \tag{20}$$

where $A_+=9\times10^{-9}$ [19,20], and the sum over all flavors of the ν and the χ is understood. Following the previous analysis for the charged lepton constraints, we obtain

$$|F_{\nu,\chi}|\lesssim 110|F_{d_1}|. \tag{21}$$

Note the bound can be stronger if more than one kind or flavor contributes.

The upper limit on $D^0\to$ invisibles by Belle [21],

$$\mathcal{B}(D^0\to\text{inv.})<9.4\times10^{-5}(90\%\,\text{C.L.}), \tag{22}$$

is, in principal, beneficial for massive invisibles (respecting $m_{\text{inv}}<m_D/2$), however, does not constrain decays to fermions with purely vectorial coupling to the Z', such as $g_4F_\chi\bar{\chi}\gamma_\mu\chi$.

4. Synopsis charm constraints and benchmarks

Charm constraints imply further selection criteria on the model charges: U-spin breaking and hierarchy $F_{d1}\gg F_{d2}$ (8), on lepton couplings (16)–(18), and on invisible and neutrino couplings (21). All benchmarks (BMs) I–IV given in Table I pass these constraints. Note that the BSM benchmarks from [10] are disfavored by the new data. BMs I and II are obtained by scanning integers. BMs III and IV are targeted toward more minimal models, with BM IV designed to have no one-loop kinetic mixing. BMs III and IV pass the additional constraints that arise from light Z' searches discussed in the next Sec. III, while BMs I and II fail to do so. BM III-s, a variant of BM III with the charges between first and second generation up-type quark singlets swapped, $F_{u1}=-F$, $F_{u2}=G$ is equally viable. It has a different phenomenology than the other BMs, as it does not couple necessarily directly to charm quarks.

Indeed the main impact from D mixing is that the mass of the Z' is light, below the weak scale. Using Eq. (5) with $F_{Q_1}=0$ and the D-mixing bound, we obtain a useful relation

$$\frac{g_4F_{d_1}}{M_{Z'}}\sim\frac{1}{0.025\ \text{TeV}}\times\frac{|a^d_{\pi^-\pi^+}|}{0.002}, \tag{23}$$

indicating a low NP mass scale, significantly lower than the naive estimate (7) due to the severe constraints from Eq. (9). The ratio of coupling over mass required to explain ΔA_{CP} alone [10] is approximately a factor of a few smaller than the one from $a^d_{\pi^-\pi^+}$ (3), due to the smaller value of the CP asymmetry and cooperating contributions from both KK and $\pi\pi$ asymmetries at least for modest U-spin breaking. The contribution of the flavorful Z' to four-quark operators $\bar{u}c\bar{q}q$, $q=d,s$ is about 2–3 orders of magnitude smaller than the one induced in the SM by W exchange. Therefore, the Z' contribution is irrelevant for the $D\to\pi^+\pi^-$ and $D\to K^+K^-$ branching ratios.

We observe that the anomaly-free models feature U-spin breaking and also isospin breaking, see Table I. This implies signal in other two-body charm CP asymmetries, such as $\pi^+\pi^0$ and $\pi^0\pi^0$, see [10] and, recently, [22]. We work out predictions in Sec. II C.

C. $A_{CP}(\pi^0\pi^0)$ and $A_{CP}(\pi^+\pi^0)$

Flavorful Z' models for ΔA_{CP} also induce CP asymmetries in the $D \to \pi^0\pi^0$ and $D \to \pi^+\pi^0$ decays [10]. They are of similar size,

$$\frac{A_{CP}(\pi^0\pi^0)}{A_{CP}(\pi^+\pi^0)} = \frac{d_{\pi^0}}{d_{\pi'}} \simeq 1.08 \pm 0.10, \tag{24}$$

and we recall that $A_{CP}(\pi^+\pi^0)$ requires isospin violation to be finite. Using $F_{d_2} \ll F_{d_1}$, we find that all CP asymmetries involving pions are generically correlated as

$$A_{CP}(\pi^+\pi^0) \simeq \frac{d_{\pi'}}{d_{\pi^0}} A_{CP}(\pi^0\pi^0) \simeq -\frac{d_{\pi'}}{d_\pi}\left(1 - \frac{F_{u_1}}{F_{d_1}}\right)\Delta A_{CP}. \tag{25}$$

Since all d_π's are roughly of the same size, and noting that viable benchmarks obey $|F_{u_1}| < |F_{d_1}|$ (see Table I and Sec. III), the Z'-induced CP asymmetries are at the level of ΔA_{CP}, which is a per mill. We also note the opposite sign of ΔA_{CP} with respect to the others, hence $A_{CP}(\pi^0\pi^0)$ and $A_{CP}(\pi^+\pi^0)$ are positive in our models. Since F_{u_1}/F_{d_1} can have either sign, the relative factor $(1 - F_{u_1}/F_{d_1})$ can be bigger or smaller than 1. Concretely, it is 1 for BM III (with $G = 0$), 2 for the twisted BM III-s (with $G = 0$), and within $1 \mp 1/\sqrt{2}$ for BM IV, depending on charges. For the BM IV solution given by Eq. (C30), we obtain a factor 1.7.

III. A FLAVORFUL Z' OF THE ORDER 10 GeV?

Because of their strong impact on the viable mass range of the Z', we begin analyzing constraints from couplings to quarks in Sec. III A. The scale required to explain charm data (23) points to a light Z'. Searches for $U(1)'$ extensions, including dark photons, B–L and B models in dileptons provide severe constraints in the 1–100 GeV range, in particular, in couplings to electrons and muons [23]. Consequently, couplings to electrons and muons, or leptons altogether, should be suppressed, much stronger than in (16) and (17). As such, BM I and II become excluded and will not be considered any further. We quantify this and constraints in Sec. III B, also working out couplings of the leptons that are induced by kinetic mixing. This effect is larger in BM III, as kinetic mixing arises here already at one loop. We analyze this and its impact in Sec. III C. In Sec. III D, we work out branching ratios of the Z'.

A. Mass constraints from $q\bar{q}$

Constraints arise from dijets. For $10 \lesssim M_{Z'} \lesssim 50$ GeV, the strongest constraints are from CMS [24] and their dijet plus initial state radiation search (ISR) [25]. Using their results, approximately $g_4 F_{d_1} \lesssim 0.5$, together with the constraint from charm (3) and (23), we arrive at the allowed mass range

$$10\ \text{GeV} \lesssim M_{Z'} \lesssim 20\ \text{GeV}. \tag{26}$$

Around and below 10 GeV, constraints depend on the benchmark models. Strong constraints from $\Upsilon \to jj$ decays exist [26] around 10 GeV. They apply to BM IV due to its $U(1)'$ charge to b quarks: If one were to charge s_R instead of b_R, the model would induce too large contributions to $D \to K^+K^-$ decays. Using Ref. [27], we obtain the allowed regions for BM IV with (C30) from $\Upsilon(1s)$ decays respecting CP data (3) and (23) as

$$M_{Z'} \lesssim 7 \quad \text{or} \quad M_{Z'} \gtrsim 15\ \text{GeV}\ (\text{BM IV}). \tag{27}$$

On the other hand, BM III and BM III-s have no Z' coupling to b's and hence evade the Υ limits.

Charmonium decays provide additional constraints below 10 GeV on BM III and BM IV, but not on the "swapped" model BM III-s, as it does not couple to charm (for $G = 0$). BM III-s with mass below (26) can be probed in low energy hadronic processes involving first generation quarks and invisibles. Because of (23) the Z' below a GeV interacts feebly. A detailed assessment of constraints and opportunities for forward facilities [28] is beyond the scope of this work.

We work out the constraints on BM III and BM IV from $\psi_i \to Z'^* \to \pi^+\pi^-$ decays, $\psi_i = J/\psi, \psi'$, with contributions illustrated in Fig. 4. Following [29], we obtain for the branching ratios normalized to the ones into electrons,

$$\frac{\mathcal{B}(\psi_i \to \pi^+\pi^-)}{\mathcal{B}(\psi_i \to e^+e^-)} \frac{4}{|F_\pi(m_{\psi_i})|^2} = |1 + A_{Z'}/A_\gamma|^2, \tag{28}$$

$$\frac{A_{Z'}}{A_\gamma} = \frac{m_{\psi_i}^2}{m_{\psi_i}^2 - M_{Z'}^2 + iM_{Z'}\Gamma(Z')} \frac{3g_4^2 F_{u2}(F_{u_1} - F_{d_1})}{8\pi\alpha_e}, \tag{29}$$

which depend on the ratio of the Z'-induced amplitude $A_{Z'}$ to the SM-photon one A_γ and the pion form factor F_π. The left-hand side of Eq. (28) is defined in such a way that by

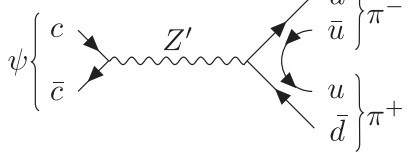

FIG. 4. Contribution of the Z' to $\psi \to \pi^+\pi^-$ amplitudes.

switching off the NP amplitude it equals 1. We employ the values of the pion form factor $|F_\pi(m_{J/\psi})| = 0.056$, $|F_\pi(m_{\psi'})| = 0.04$ from [30], which uses data on $e^+e^- \to \pi^+\pi^-$ and pion-electron scattering as input. As our models are electrophobic, we can safely assume that these data are not affected by the Z'. The Z' width $\Gamma(Z')$ is obtained from (44).

The constraints on BM III are shown in Fig. 5 (top) and for BM IV with (C30) (bottom). The gray line denotes the SM prediction corresponding to the ratios in (28) being equal to 1. One notices that the NP contribution decouples very slowly for larger Z' masses; the reason is the growth of coupling with mass by means of (23). We also include the experimental uncertainties from the CP data (3). The main difference between the models BM III and BM IV is stemming from the $\gamma - Z'$-interference term, which has opposite sign but similar size. We observe for BM III that Z' masses around [2.3, 2.8] and [3.2, 3.5] GeV are consistent with both the J/Ψ data (red horizontal bands) and the charm anomalies (red curves). The ranges obtained using ψ' data (blue horizontal bands), which have larger uncertainties, are [1.9, 3.3] or [3.9, 4.5] GeV. BM IV can

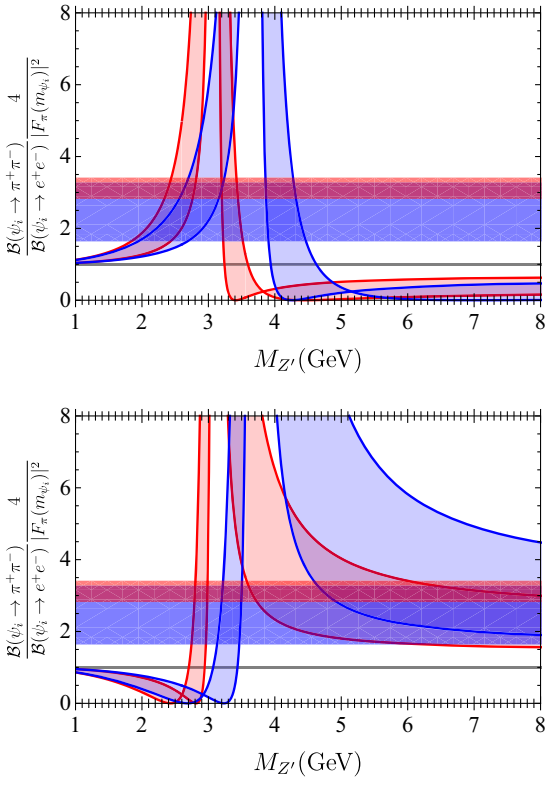

FIG. 5. Constraints from charmonium decays. Horizontal red (blue) bands denote the left-hand side of (28) from 1 sigma ranges of J/ψ data with $|F_\pi(m_{J/\psi})| = 0.056$ [ψ' decays with $|F_\pi(m_{\psi'})| = 0.04$]. Values of the pion form factor are from [30]. Curves correspond to the predictions [right-hand side of (28)] in BM III with $F \gg G$ (top) and BM IV with (C30) (bottom) using (23), including experimental uncertainties from (3). The SM prediction via photon exchange is shown by the gray line.

explain charm CP data and $J/\psi \to \pi\pi$ decays for masses within [2.8, 3.0] GeV or starting from 3.6 GeV until the Υ limit (27) kicks in, at about 7 GeV. The corresponding ranges from the ψ' data read [3.1, 3.5] or [4.6, 7] GeV. Assuming compatibility with both charmonia [31], Υ and charm CP data determine the Z' mass, depending on the model, as

$$M_{Z'} \sim [2.3, 2.8] \quad \text{or} \quad [3.2, 3.3]\ \text{GeV (BM III)},$$
$$M_{Z'} \sim [4.6, 7]\ \text{GeV (BM IV)}. \tag{30}$$

With these parameters, our models provide an opportunity to resolve the longstanding tension between F_π extracted from J/ψ decays assuming the leading photon-exchange contribution and QCD, e.g., [32]. Note that the explanation of charmonia in BM III is a resonant effect, while in BM IV it is in the tails.

We recall that our results are subject to sizable uncertainties: the weak effective theory is challenged since a Z' as light as a few GeV is close to the charm scale, in addition to the uncertainties from hadronic matrix elements. We also neglect G-parity-violating contributions in the SM to the charmonia decays, e.g., [33], noting that the tension is significant, 7σ for the J/π and 1.8σ for the ψ'. As such, we consider the phenomenology and formal constraints also in wider viable regions of $M_{Z'}$.

For BM III, additional constraints from charmonia to taus or invisibles exist. Using a similar computation as in (28), we find that $\mathcal{B}(\psi' \to \tau^+\tau^-)$ [31] gives the allowed mass ranges $M_{Z'} \lesssim 2.2$ GeV or within $4.0 - 4.8$ GeV, very close to the windows implied by the pion form factor (30). In view of the large uncertainties further analyses are promising and desirable. Furthermore, $\mathcal{B}(\psi \to \text{nothing}) < 7 \cdot 10^{-4}$ [31] requires either $M_{Z'} \lesssim 0.7$ GeV, which is in conflict with (30), or the BSM neutrino which couples to the Z' to be heavier than half the ψ mass to forbid the decay kinematically. This suggests that this benchmark solution to the charm CP-data can be probed in charmonium decays.

B. $Z' \to ee$ and $\mu\mu$ bounds

We work out constraints from $Z' \to e^+e^-, \mu^+\mu^-$ decay searches. First, we study models where the Z' couples directly to electrons or muons [34,35], such as BM I–III (with $G \neq 0$) and IV,

$$g_4 F_{e_i,L_i} = \sqrt{8\pi\alpha_e}\varepsilon \approx 0.4\varepsilon. \tag{31}$$

The experimental search limits are given in terms of the mixing parameter ε, defined as $\mathcal{L}_\varepsilon = -\varepsilon e J^\mu Z'_\mu$, where J^μ is the electromagnetic current of SM fermions. For the range of interest (40), the current experimental limit on ε both for electrons and muons is [23,36]

$$|\varepsilon(M_{Z'})| \lesssim 10^{-3}. \tag{32}$$

Combining Eq. (31) with (32), one gets

$$g_4 F_{e_{1,2},L_{1,2}} \lesssim 4 \times 10^{-4}. \tag{33}$$

Inspecting Fig. 3, we observe that $g_4 F_{d_1} \gtrsim 0.3$ for $M_{Z'} \gtrsim 10$ GeV, which in combination with Eq. (33) leads to a strong suppression of electron and muon couplings over the down-type quark one,

$$\frac{F_{e_{1,2},L_{1,2}}}{F_{d_1}} \lesssim \frac{1}{750}, \tag{34}$$

significantly stronger than the rare D decay and Drell-Yan constraints (16) and (17). Note that Eq. (34) directly excludes BM I and II and dictates a strong quark and lepton charge hierarchy in BM III (as $|G| \lesssim 1.3 \times 10^{-3}|F|$) and IV.

Next, we study effects from kinetic mixing. If the Z' does not couple directly to electrons and muons as in BM III with $G = 0$, one can still induce a small coupling ε to $\mathcal{L}_\varepsilon$ from $Z' - \gamma$ gauge-kinetic mixing,

$$\mathcal{L} \supset -\frac{1}{4} F^{\mu\nu} F_{\mu\nu} - \frac{1}{4} Z'^{\mu\nu} Z'_{\mu\nu} - \frac{\eta}{2} F^{\mu\nu} Z'_{\mu\nu}, \tag{35}$$

which yields

$$\varepsilon = -\frac{\eta}{\sqrt{1-\eta^2}}. \tag{36}$$

Note that gauge-kinetic mixing is, in general, not technically natural and cannot be switched off at more than one scale. It is also related to the gauge-kinetic mixing between the Z' and the hypercharge field B before electroweak symmetry breaking via $\eta = \eta_{B-Z'} \cos\theta_W$. This implies $Z - Z'$ mass mixing, generating a correction δM_Z to the unmixed tree-level mass of the Z boson, which affects the ρ parameter $\rho^{-1} = (M_Z + \delta M_Z)\cos\theta_W / M_W$,

$$\left(\frac{\rho - \rho_{\mathrm{SM}}}{\rho}\right) = -\frac{\varepsilon^2 \tan^2\theta_W}{2(1+\varepsilon^2)} \left(\frac{M_{Z'}}{M_Z}\right)^2 + \mathcal{O}\left(\frac{M_{Z'}}{M_Z}\right)^4, \tag{37}$$

which for light Z''s is negative, but vanishes quadratically with ε. Here, ρ_{SM} denotes the ρ parameter's SM value, which is close to 1. The global fit of electroweak precision parameters [31] suggests a relative NP contribution as

$$\left(\frac{\rho - \rho_{\mathrm{SM}}}{\rho}\right) = (3.8 \pm 2.0) \times 10^{-4}. \tag{38}$$

Thus, the light Z' contributes with the opposite sign. However, the correction is within 2σ of (38) if

$$|\varepsilon(M_Z)| \lesssim 4 \times 10^{-1} \quad (7 \times 10^{-2}), \tag{39}$$

for a Z' mass above 3 GeV (15 GeV). This has to be compatible with the constraint (32) at the $M_{Z'}$ scale. As the running of ε is, in general, not technically natural, avoiding both constraints may result in highly nontrivial conditions of all $U(1)'$ charges for a light Z'. In the following section, we discuss benchmark models that are feasible in this regard.

C. Viable scenarios

We consider the benchmarks BM III and BM IV, see Table I, which allow for sizable couplings to quarks but not leptons (34). Note that in these models the top quark has no direct coupling to the $U(1)'$. This is also beneficial in suppressing contributions from kinetic mixing.

(A) BM IV follows the constructions of Appendix C, with $|F_e| \ll |F_{u,d}|$. The kinetic mixing is natural in this model and can be switched off or made feebly small, see Appendix D.

(B) BM III is electron- and muophobic. It has couplings to taus and ν_R. The RG evolution of the kinetic mixing parameter reads

$$\varepsilon(\mu) = \varepsilon(\mu_0) - \delta_\varepsilon \ln\left(\frac{\mu}{\mu_0}\right) + \text{2-loop}, \tag{40}$$

$$\delta_\varepsilon = \frac{e g_4 F}{3\pi^2} + \mathcal{O}(\varepsilon). \tag{41}$$

As

$$g_4(M_{Z'}) F \gtrsim \frac{30 M_{Z'}}{\mathrm{TeV}}, \tag{42}$$

see Fig. 3, we roughly find a running

$$|\varepsilon(M_Z) - \varepsilon(M_{Z'})| \gtrsim \frac{10e}{\pi^2} \frac{M_{Z'}}{\mathrm{TeV}} \ln\left(\frac{M_Z}{M_{Z'}}\right) \gtrsim 10^{-3} \tag{43}$$

between the Z' and the electroweak scale, where in the last line of (43) we used $M_{Z'} \gtrsim 3$ GeV. Thus, the running can accommodate both ρ parameter and $Z' \to \ell\ell$ constraints (32) and (39) if $|\varepsilon(M_Z)| \sim \mathcal{O}(10^{-2})$. Using the four-loop running [37,38], we verified that the approximation (40) holds well for the lower end of (42). Larger values of $g_4(M_{Z'})F$ may result in (43) increasing in the order of magnitude, eventually spoiling compatibility with the kinetic mixing constraints.

To summarize, bounds from ee and $\mu\mu$ can always be evaded: In BM IV, the hierarchy between quark and lepton charges can simply be chosen larger. In BM III, while kinetic mixing induces couplings to SM fermions that are uncharged before going to the gauge boson mass basis, the impact of this can be avoided by tuning with the contribution at the matching scale (40), at the level of 0.1.

If experimental dilepton constraints on ε improve in the future, this can be accommodated with an increase of tuning at similar level. Of course, in a UV model this choice is not possible, therefore, models of type BM III can be just around the corner and show up in the next round of dilepton searches.

D. Z' decay

In this section, we work out branching ratios of the light Z' boson. The partial decay width of the Z' to fermions ψ with mass $m_\psi < M_{Z'}/2$ is given as [35]

$$\Gamma(Z' \to \psi\bar{\psi}) = \frac{N_C^\psi g_4^2}{24\pi} M_{Z'} \sqrt{1-4\frac{m_\psi^2}{M_{Z'}^2}} \cdot \left[F_{\psi_L}^2 + F_{\psi_R}^2 - \frac{m_\psi^2}{M_{Z'}^2}(F_{\psi_L}^2 - 6F_{\psi_L}F_{\psi_R} + F_{\psi_R}^2)\right], \tag{44}$$

with color factor $N_C^\psi = 3$ for quarks and $N_C^\psi = 1$ otherwise. $F_{\psi_{L(R)}}$ denotes the $U(1)'$ charge of the left-handed (right-handed) fermion ψ. Because of the low mass of the Z' (26) decay channels into the SM electroweak gauge bosons or the Higgs are kinematically forbidden. For low $M_{Z'} \lesssim$ few $\times$ GeV, also the fermionic decays $Z' \to b\bar{b}, c\bar{c}, \tau^+\tau^-$ can be either kinematically forbidden or severely phase space suppressed. In the limit $m_\psi^2/M_{Z'}^2 \ll 1$, on the other hand, the branching ratios are simply given by

$$\mathcal{B}(Z' \to \psi\bar{\psi}) = \frac{N_C^\psi(F_{\psi_L}^2 + F_{\psi_R}^2)}{\sum_{\psi'} N_C^{\psi'}(F_{\psi'_L}^2 + F_{\psi'_R}^2)}. \tag{45}$$

Numerical results for branching ratios in BM III, III-s, and IV are shown in Table II for different $M_{Z'}$. In BM III and III-s, results are given in the limit $G \ll F$ where dimuon bounds are avoided. For $M_{Z'} = 20$, 10, and 3 GeV using (23) in BM III we obtain the width $\Gamma(Z') = \sum_i \Gamma(Z' \to \psi_i\bar{\psi}_i)\theta(M_{Z'} - 2m_{\psi i}) = 1.8$, 0.2 and 4×10^{-3} GeV, respectively. Very similar values for $\Gamma(Z')$ are found in BM III-s and IV. We note that for the lower masses Eq. (44) is not accurate as hadronic final states should rather be taken into account. In BM IV, results depend on the charge assignments $F_{u,d,e,\nu}$. However, dilepton bounds suggest suppression of lepton couplings (34). When setting $|F_e|, |F_\nu| \ll |F_{u,d}|$ we asymptotically approach a leptophobic model, with decays only to b, c, and jets, i.e., light quarks. We also provide branching ratios for the concrete scenario (C30) in Table II. All benchmark models lead to a promptly decaying Z'.

Another possibility to suppress branching ratios to quarks and charged leptons is $|F_\nu| \gg |F_{u,d,e}|$. In this case, the Z' boson decays mostly invisibly to right-handed neutrinos. The same effect can also be achieved in all BMs by adding a light and dark vectorlike BSM fermion χ with $U(1)'$ charge F_χ. Because of its vectorlike nature, χ does not contribute to any gauge anomalies and it can have a simple Dirac mass term. Assuming $m_\chi < 2M_{Z'}$ as well as $|F_\chi| \gtrsim |F_\psi|$ for $\psi = Q, u, d, L, e, \nu$, the Z' will decay predominantly invisibly as $Z' \to \chi\bar{\chi}$, see (45). For a heavy Z' this possibility has already been explored in the context of the B anomalies [35]. The Z' can be radiated off quarks, which in the above scenario leads to characteristic signatures such as hadrons in association with invisibles, i.e., missing energy, see Fig. 6. Unfortunately, to our knowledge, in the mass range of our interest, there is no experimental analysis for this process available. However, an invisibly decaying Z' radiated off final state hadrons would be the smoking gun signature of this scenario at e^+e^- machines, potentially giving rise to tight

TABLE II. Tree-level branching fractions in percentage for the different Z' decay modes to fermion-antifermion pairs. Results for BM III and BM III-s are given in the limit $G \ll F$. In BM IV, branching ratios depend on the different charge assignments $F_{u,d,e,\nu}$, see main text for details. The branching ratios shown in this table are obtained from $F_u = 985$, $F_d = 1393$, $F_e = 1$ in (C30), and $F_\nu = 0$. Branching ratios in all BMs differ perceptibly between the low and high $M_{Z'}$ windows, (26) and (30), as the decays $Z' \to b\bar{b}, c\bar{c}, \tau^+\tau^-$ are kinematically forbidden or suppressed in the few GeV range. Corrections to branching ratios from kinetic mixing are generically $\lesssim 10^{-7}$.

Model	Light quarks	b	c	e	μ	τ	ν_R
BM III$\vert_{M_{Z'}=2.5\text{ GeV}}$	75	0	0	0	0	0	25
BM III$\vert_{M_{Z'}=15\text{ GeV}}$	38	0	37	0	0	12	13
BM III-s$\vert_{M_{Z'}=2.5\text{ GeV}}$	86	0	0	0	0	0	14
BM III-s$\vert_{M_{Z'}=15\text{ GeV}}$	75	0	0	0	0	12	13
BM IV$\vert_{M_{Z'}=5\text{ GeV}}$	79	0	21	0	0	0	0
BM IV$\vert_{M_{Z'}=15\text{ GeV}}$	54	28	18	0	0	0	0

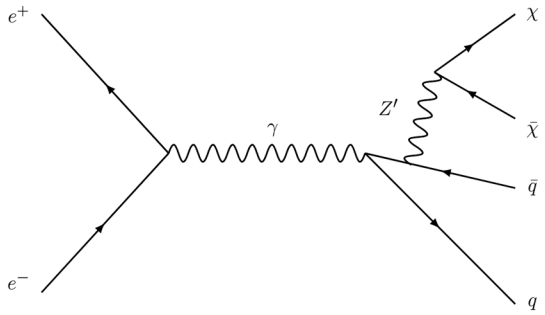

FIG. 6. Smoking gun signature of benchmark models at e^+e^- machines for $|F_{\nu/\chi}| \gtrsim |F_\psi|$ where $\psi = Q, u, d, L, e, \nu$. A $q\bar{q}$ pair is produced via an s-channel photon and radiates of a Z' invisibly decaying to $\chi\bar{\chi}$ or $\nu\bar{\nu}$, leading to a final state containing hadrons in association with missing energy.

bounds on $F_{\nu\chi}$. This is in contrast to bounds from existing searches for $e^+e^- \to \gamma_{\rm ISR} + (Z' \to \chi\bar{\chi})$ [39–41], where cross sections are suppressed by tiny factors ε^2 or F_e^2 even if $\mathcal{B}(Z' \to \chi\bar{\chi}) \simeq 100\%$. However, note that $F_{\nu,\chi}$ cannot be arbitrarily large, as by adding additional $U(1)'$-charged matter we always increase the RG growth of g_4, which finally might give rise to a low energy Landau pole, see Sec. IV for details. There are also constraints (21) on the charges from rare decays for fermions lighter than $m_D/2$.

We comment on corrections to the Z' decay rate to SM fermions from kinetic mixing. As discussed in III B, the Z' thus couples to the electromagnetic current J^μ via $\mathcal{L}_\varepsilon = -\varepsilon e J^\mu Z'_\mu$, where the kinetic mixing parameter ε is defined in (35) and (36). The corresponding partial decay width can be obtained from (45) by replacing $g_4 \to \varepsilon e$ and the $U(1)'$ charges with electric ones, $F_{\psi_{L,R}} \to q_\psi$. Experimentally, kinetic mixing is constrained by (32) to be small. Thus, decays via kinetic mixing are suppressed in comparison to unmixed decays by a tiny factor,

$$\kappa \sim \frac{\sum_\psi (2N_C^\psi q_\psi^2)\varepsilon^2 e^2}{\sum_\psi N_C^\psi (F_{\psi_L}^2 + F_{\psi_R}^2) g_4^2} \propto \frac{\varepsilon^2 e^2}{g_4^2}, \tag{46}$$

where we rescaled the $U(1)'$ charges and coupling such that $\max(F_{\psi_{L/R}}) = 1$. Then, to create the desired value (3) of $a^d_{\pi^+\pi^-}$, it follows from (23) that $g_4 \gtrsim \mathcal{O}(1)$ for the Z' mass range given by (26). Putting everything together, we obtain $\kappa \lesssim 10^{-7}$. This provides an order of magnitude estimate for the branching ratios into $U(1)'$-uncharged fermions.

IV. HIGH ENERGY BEHAVIOR

Let us investigate the consequences of (23) for the consistency of the $U(1)'$ gauge group at higher energies. We by begin asking about perturbativity. Using

$$g_4 F_\psi \lesssim 4\pi, \tag{47}$$

for all SM fields ψ the Z' mass gets bounded from above,

$$M_{Z'} \lesssim 400 \text{ GeV}. \tag{48}$$

Next, we investigate the occurrence of Landau poles (LPs). Neglecting kinetic mixing effects, the scale $\mu_{\rm LP}$ of the $U(1)'$ pole can be estimated as

$$\mu_{\rm LP} = \mu \cdot \exp\left[\frac{(4\pi)^2}{g_4^2(\mu) B_4}\right], \tag{49}$$

with the one-loop coefficient in the beta-function

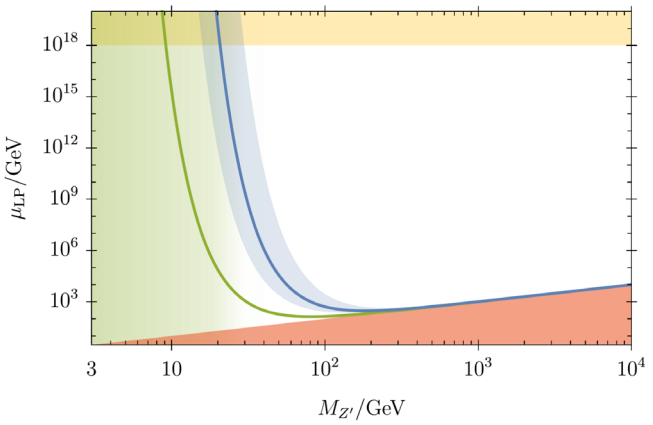

FIG. 7. Scale of the Landau pole $\mu_{\rm LP}$ via the estimate (52) for BM III (blue), depending on the $M_{Z'}$ mass. An uncertainty of 30% is considered for $a^d_{\pi^-\pi^+}$ in (23), consistent with (3) (blue-shaded area). The shifted central value is also shown if one dark fermion $F_\chi = 4F$ is included (solid green line). The red-shaded area is excluded, as $\mu_{\rm LP} \leq M_{Z'}$. The preferred mass range (26) of $M_{Z'}$ is shaded in green. The yellow band indicates the $\mu_{\rm LP}$ regime an order of magnitude around the Planck scale.

$$B_4 = \sum_\psi \frac{4}{3} d_2(\psi) d_3(\psi) F_\psi^2, \tag{50}$$

counting over all Weyl fermions ψ. The corresponding gauge coupling g_4 is fixed by data, e.g., (23), at the scale of NP $\mu = M_{Z'}$. One obtains schematically

$$\frac{g_4(M_{Z'})}{M_{Z'}} = \frac{1}{\sqrt{B_4} m_0}, \tag{51}$$

with m_0 being a characteristic mass scale. Thus, the scale of the Landau pole is around

$$\mu_{\rm LP} = M_{Z'} \cdot \exp\left[\frac{(4\pi)^2 m_0^2}{M_{Z'}^2}\right]. \tag{52}$$

For large-Z' masses $M_{Z'} \gg 4\pi m_0$ this implies $\mu_{\rm LP} = M_{Z'}$. Nearby Landau poles can hence only be avoided if $M_{Z'} \ll 4\pi m_0$.

In Fig. 7, the location of the Landau pole with respect to $M_{Z'}$ is illustrated for BM III, where $B_4 = \frac{32}{3}F^2$ and (42) imply $m_0 \approx 10$ GeV. Shown are the central value for $\mu_{\rm LP}$ (blue line), a 30% uncertainty band for $a^d_{\pi^-\pi^+}$ in (23), consistent with (3) (blue-shaded area), and the shifted central value due to a dark fermion (with $F_\chi = 4F$, solid green line).[3] The red-shaded area ($\mu_{\rm LP} \leq M_{Z'}$) is excluded. We observe that the Landau pole may be beyond the Planckian regime (yellow band) only for very light Z'

[3]With N_χ additional vectorlike, $U(1)'$-charged dark fermions χ, see Sec. III D, B_4 increases by $\delta B_4 = \frac{8}{3}F_\chi^2 N_\chi$.

($M_{Z'} \lesssim 20$ GeV, green-shaded area) and sub-Planckian otherwise. Increasing $M_{Z'}$, the Landau pole decreases toward a TeV-ish minimum (where $M_{Z'} \gtrsim 81$ GeV), implying an upper bound for $M_{Z'}$. For $M_{Z'}$ beyond the electroweak scale, the Landau pole stays exponentially close to $M_{Z'}$, indicating that the theory is strongly coupled. Finally, we note that the addition of extra $U(1)'$ charge carriers, e.g., a dark fermion, shifts the Landau pole toward lower values and more substantially so for low $M_{Z'}$.

This overall pattern is in sharp contrast to the situation observed in rare b decays, where the anomalies indicate $\sqrt{B_4} m_0 \simeq 40$ TeV and a TeV-size Z' is vastly separated from the Landau pole. This permits the introduction of additional BSM interactions to evade the Landau pole and to secure Higgs stability all the way up to the Planck scale (and possibly beyond) [35].

Finally, we emphasize that a sub-TeV-ish Landau pole is avoided as long as

$$M_{Z'} \lesssim \text{few} \times 10 \text{ GeV}, \tag{53}$$

consistent with search limits (26) and $q\bar{q}$ data (27) and (30).

V. CONCLUSIONS

The recent data on charm CP violation (1), taken at face value, together with the measurement of ΔA_{CP} (2), require one to accept a huge amount of U-spin breaking or NP below the weak scale. Explaining Eq. (3) indeed poses a challenge to model building, given the low NP scale and the severe constraints from rare decays, mixing, and searches for BSM bosons in dilepton and dijets channels.

We obtain viable explanations of data (3) from a light Z' boson, $M_{Z'} < \text{few} \times 10$ GeV, with novel, characteristic patterns in couplings to fermions: successful model benchmarks, see Table I, accidentally couple only to right-handed fermions and are leptophobic (BM IV) or do not have $U(1)'$ charges to electrons or muons (BM III). The latter is subject to kinetic mixing at one loop, which requires a nonexcessive tuning of the mixing parameter at the level of 10%. The former is a novel benchmark using a Diophantine construction to maintain anomaly freedom and the absence of one-loop kinetic mixing, since it couples mostly to quarks without introducing new matter fields, derived in Appendix C.

Models do not couple to top quarks, allowing for the top Yukawa to be written down directly. BM III allows also the bottom Yukawa at tree level. We stress that we are not addressing the origin of flavor, which is beyond the scope of this work. Models can also include a dark sector, which can significantly speed up the running such that low scale Landau poles arise that point to a UV completion as low as a TeV, see Fig. 7. However, in view of the "the lighter, the safer" rule, a sufficiently light Z', with details depending on the dark sector, can avoid this.

Model frameworks BM III and BM IV are unique, as they are minimal models passing the very many theoretical and experimental constraints. Together with viable variants obtained by swapping charges within one species, such as BM III-s, they are indeed the only, minimal options, inducing CP violation in the $\bar{c}_R u_R$ current and an enhanced $\bar{d}_R d_R$ current, but it cannot be ruled out that further, highly tuned scenarios with crosstalk between species may be constructed. Another intriguing feature of the models is that they can simultaneously explain the charm CP data (3) and the $J/\psi \to \pi^+\pi^-$, $\psi' \to \pi^+\pi^-$ branching ratios for a Z' around $\sim$3 GeV (BM III) or $\sim$(5–7) GeV (BM IV), see Sec. III A, providing a NP explanation to the long-standing pion form factor puzzle.

Models can be searched for in low mass dijets along the lines of [24] or Υ and J/ψ or ψ' decays and related dark photon searches. The dominant Z' branching ratios are given in Table II. Signatures include enhanced production in $\pi^+\pi^-$, or DD, and $\tau\tau$ in BM III. If dark fermions are also present, signatures as in Fig. 6 with hadrons and invisibles are promising smoking guns. We stress that BM III-s, a variant of BM III with the charges between first and second generation up-type quark singlets flipped, $F_{u1} = -F$, $F_{u2} = G$ is equally viable. It has a different phenomenology than the other benchmark models, as it does couple essentially to first generation quarks, the τ, and neutrinos, hence evades charmonium limits and could be as light as $\mathcal{O}(\text{GeV})$ or possibly below.

All viable models further predict isospin violation and pattern in the CP asymmetries in hadronic charm decays, see (25), in addition to $A_{CP}(D \to K_S K_S)$, which also requires U-spin breaking [11]. Models are tightly constrained by D mixing and Z' searches into electrons and muons. They can hence signal NP in the next round of data.

ACKNOWLEDGMENTS

We are happy to thank Tommaso Pajero and Stefan Schacht for useful communication, and Alex Gilman for pointing out charmonia bounds for taus and invisibles. This work is supported by the Studienstiftung des Deutschen Volkes (TH), the Bundesministerium für Bildung und Forschung (BMBF) under Project No. 05H21PECL2 (H. G.), and the Science and Technology Research Council (STFC) under the Consolidated Grant No. ST/T00102X/1 (D. F. L.). This work was performed in part at Aspen Center for Physics (G. H., D. F. L.), which is supported by National Science Foundation Grant No. PHY-1607611, and was partially supported by a grant from the Simons Foundation (D. F. L.). G. H. is grateful to the MITP of the PRISMA$^+$ Cluster (Project ID 39083149) for its hospitality and partial support during the completion of this work.

APPENDIX A: AMPLITUDES AND OBSERVABLES IN SM

The SM decay amplitudes of $D \to \pi^+\pi^-$ and its conjugate decay can be written in terms of reduced amplitudes t, h with relative strong phase δ as

$$A = A(D^0 \to \pi^+\pi^-)^{\mathrm{SM}} = \Sigma t + V_{cb}^* V_{ub} h e^{i\delta}, \tag{A1}$$

$$\bar{A} = A(\bar{D}^0 \to \pi^+\pi^-)^{\mathrm{SM}} = \Sigma^* t + V_{cb} V_{ub}^* h e^{i\delta}, \tag{A2}$$

where $\Sigma = (V_{cd}^* V_{ud} - V_{cs}^* V_{us})/2$ and $V_{cs}^* V_{us} \simeq -V_{cd}^* V_{ud}$ due to CKM unitarity up to a negligible $V_{cb}^* V_{ub}$. The amplitude t is predominantly induced by tree-level W exchange, whereas h originates from higher-order contributions including penguin loops or final state interactions. Using standard formulas, one obtains for the direct CP asymmetry of $D \to \pi^+\pi^-$ decays in the SM,

$$a_{\pi^-\pi^+}^{d\mathrm{SM}} = \frac{|A|^2 - |\bar{A}|^2}{|A|^2 + |\bar{A}|^2} \simeq 2 \cdot \mathrm{Im}\left(\frac{V_{cb}^* V_{ub}}{V_{cd}^* V_{ud}}\right) \frac{h}{t} \sin\delta, \tag{A3}$$

where we neglected contributions of higher order in CKM ratios $V_{cb}^* V_{ub}/(V_{cd}^* V_{ud}) \sim 10^{-3}$. This approximation implies also that the CP-averaged branching ratio is dominated by the term with the leading CKM factor Σ, $\mathcal{B}(D \to \pi^+\pi^-) \propto |A|^2 + |\bar{A}|^2 \propto |\Sigma|^2 t^2$.

Expressions for $D \to K^+K^-$ decays are analogous,

$$A(D^0 \to K^+K^-)^{\mathrm{SM}} = -\Sigma t_s + V_{cb}^* V_{ub} h_s e^{i\delta_s}, \tag{A4}$$

$$A(\bar{D}^0 \to K^+K^-)^{\mathrm{SM}} = -\Sigma^* t_s + V_{cb} V_{ub}^* h_s e^{i\delta_s}. \tag{A5}$$

In the U-spin limit, the phase and reduced amplitudes are universal, such as $t = t_s = \bar{t}$ and so on. The observed U-spin breaking in the branching ratios $\mathcal{B}(D \to K^+K^-)/\mathcal{B}(D \to \pi^+\pi^-) \simeq 2.8$ can be explained with a flavor-dependent correction δt, as $t_s = \bar{t} + \delta t$, $t = \bar{t} - \delta t$ at the nominal level of flavor breaking, $\delta t/\bar{t} \simeq 30\%$ [6]. This U-spin breaking in the branching ratios and correspondingly between the leading contributors to the amplitudes t, t_s implies a shift in the CP asymmetries, e.g., (A3) and leads to the modified U-spin relation (4).

APPENDIX B: RGE AND HADRONIZATION

NP effects in charm decays are described within the effective weak Hamiltonian $\mathcal{H}_{\mathrm{eff}}^{|\Delta c|=1} \supset \frac{G_F}{\sqrt{2}} \sum_i \tilde{C}_i^{(\prime)} \tilde{Q}_i^{(\prime)}$. Operators relevant to a Z'-boson coupling to right-handed quarks read

$$\tilde{Q}'_9 = (\bar{u}c)_{V+A} \sum_q F_{u_i,d_i} (\bar{q}q)_{V+A}, \tag{B1}$$

$$\tilde{Q}'_{10} = (\bar{u}_\alpha c_\beta)_{V+A} \sum_q F_{u_i,d_i} (\bar{q}_\beta q_\alpha)_{V+A}, \tag{B2}$$

where $(V \pm A)$ refers to the Dirac structures $\gamma_\mu(1 \pm \gamma_5)$, $q = u, c, d, s, b$, and α, β are color indices.

In the following, we address the evolution of the Wilson coefficients at the Z' mass scale,

$$\tilde{C}'_9(M_{Z'}) = \frac{\sqrt{2}}{G_F} \Delta\tilde{F}_R \frac{g_4^2}{4M_{Z'}^2} e^{i\Phi_R}, \qquad \tilde{C}'_{10}(M_{Z'}) = 0, \tag{B3}$$

down to the charm mass scale at leading order in α_s, see [10] for details. The CP violating phase is $\Phi_R \sim \pi/2$. Using the anomalous dimension given by Eq. (B1) in Ref. [10] and integrating out degrees of freedom at the (Z', t, b) scales, one obtains

$$\vec{C}(\mu) = U(\mu, M_{Z'}) \vec{C}(M_{Z'}), \tag{B4}$$

where $U(m_1, m_2)$ is the evolution matrix from scale m_2 to scale m_1. Using Eqs. (B3) and (B4), we obtain

$$\tilde{C}'_9(m_c) = \frac{1}{2}\left(R^{\frac{1}{2}} + R^{-1}\right) \tilde{C}'_9(M_{Z'}), \tag{B5}$$

$$\tilde{C}'_{10}(m_c) = \frac{1}{2}\left(R^{\frac{1}{2}} - R^{-1}\right) \tilde{C}'_9(M_{Z'}), \tag{B6}$$

where

$$R = \left(\frac{\alpha_s^{(4)}(m_b)}{\alpha_s^{(4)}(m_c)}\right)^{\frac{12}{25}} \left(\frac{\alpha_s^{(5)}(m_t)}{\alpha_s^{(5)}(m_b)}\right)^{\frac{12}{23}} \left(\frac{\alpha_s^{(6)}(M_{Z'})}{\alpha_s^{(6)}(m_t)}\right)^{\frac{4}{7}}, \tag{B7}$$

for $M_{Z'} > m_t$, while

$$R = \left(\frac{\alpha_s^{(4)}(m_b)}{\alpha_s^{(4)}(m_c)}\right)^{\frac{12}{25}} \left(\frac{\alpha_s^{(5)}(M_{Z'})}{\alpha_s^{(5)}(m_b)}\right)^{\frac{12}{23}}, \tag{B8}$$

for $m_b \le M_{Z'} \le m_t$.

For the computation of the $D^0 \to K^+K^-$ and $D^0 \to \pi^+\pi^-$ hadronic matrix elements, we employ factorization of currents,

$$\begin{aligned}&\langle P^+P^-|Q_i|D^0\rangle \\ &\quad = \langle P^+|(\bar{q}_1\Gamma_1 q_2)|0\rangle \langle P^-|(\bar{q}_3\Gamma_2 q_4)|D^0\rangle B_i^{P^+P^-},\end{aligned} \tag{B9}$$

with $P = \pi, K$, $Q_i = (\bar{q}_1\Gamma_1 q_2)(\bar{q}_3\Gamma_2 q_4)$ is a four-quark operator, and $\Gamma_{1,2}$ represent Dirac and color structures, while q_j denote quarks. The factor $B_i^{P^+P^-}$ parametrizes the

deviation of the true hadronic matrix element from its naïve approximation, $B_i^{P^+P^-}|_{\text{naïve}} = 1$. Including these effects, the CP asymmetries become

$$a^d_{K^-K^+} \propto F_{d_2}\left(\frac{\tilde{C}'_9(m_c)}{N_C}B_9^{K^-K^+} + \tilde{C}'_{10}(m_c)B_{10}^{K^-K^+}\right),$$
$$a^d_{\pi^-\pi^+} \propto F_{d_1}\left(\frac{\tilde{C}'_9(m_c)}{N_C}B_9^{\pi^-\pi^+} + \tilde{C}'_{10}(m_c)B_{10}^{\pi^-\pi^+}\right), \quad \text{(B10)}$$

where we have already used $F_{Q_{1,2}} = 0$. Furthermore,

$$d_K = \frac{1}{a_K}r_2^K(m_c, M_{Z'}), \quad d_\pi = -\frac{1}{a_\pi}r_2^\pi(m_c, M_{Z'}), \quad \text{(B11)}$$

with

$$r_2^P(m_c, M_{Z'}) = \frac{B_+^P R^{1/2} - B_-^P R^{-1}}{\sqrt{2}G_F\lambda_s}, \quad \text{(B12)}$$

and

$$B_\pm^P = \frac{1}{2}\left(B_{10}^{P^+P^-} \pm \frac{1}{N_C}B_9^{P^+P^-}\right). \quad \text{(B13)}$$

In naïve factorization, $B_+^P = 2/3$ and $B_-^P = 1/3$, recovering Eq. (D2) from Ref. [10]. In the large-N_C limit $B_\pm^P = (1/2)B_{10}^{P^+P^-}$. We show d_π against $M_{Z'}$ in Fig. 8. In naive factorization (red lines) d_π exhibits a strong cancellation around ∼40 GeV stemming from the numerator of Eq. (B12). Comparing with the large-N_C limit (green lines), we observe that this cancellation is only effective in the naïve factorization limit. Taking into account that naïve factorization suffers from sizable uncertainties, blue lines illustrate 30%, in our analysis for light Z' masses we use $d_\pi \simeq 0.1$ TeV^2.

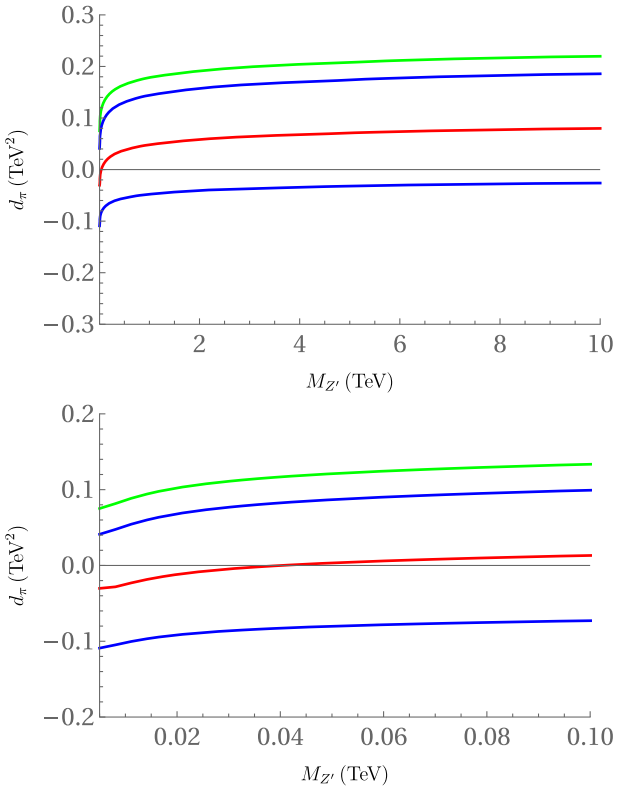

FIG. 8. d_π as a function of $M_{Z'}$ as in (B11) and (B12). The red line is obtained for $B_{9,10}^{\pi^+\pi^-} = 1$, that is, the naïve factorization approach. Here, d_π crosses zero around 40 GeV. Blue lines account for a deviation of 30% from the naïve factorization limit, that is, $B_{9,10}^{\pi^+\pi^-} = 1 \pm 0.3$. The green line represents the large-N_C limit.

APPENDIX C: ANOMALY CANCELLATION

The gauge anomaly cancellation conditions (ACCs) read [42,43]

$$2\langle\mathcal{F}_Q\rangle - \langle\mathcal{F}_u\rangle - \langle\mathcal{F}_d\rangle = 0, \quad \text{(C1)}$$

$$3\langle\mathcal{F}_Q\rangle + \langle\mathcal{F}_L\rangle = 0, \quad \text{(C2)}$$

$$\langle\mathcal{F}_Q\rangle + 3\langle\mathcal{F}_L\rangle - 8\langle\mathcal{F}_u\rangle - 2\langle\mathcal{F}_d\rangle - 6\langle\mathcal{F}_e\rangle = 0, \quad \text{(C3)}$$

$$6\langle\mathcal{F}_Q\rangle + 2\langle\mathcal{F}_L\rangle - 3\langle\mathcal{F}_u\rangle - 3\langle\mathcal{F}_d\rangle - \langle\mathcal{F}_e\rangle - \langle\mathcal{F}_\nu\rangle = 0, \quad \text{(C4)}$$

$$\langle\mathcal{F}_Q^2\rangle - \langle\mathcal{F}_L^2\rangle - 2\langle\mathcal{F}_u^2\rangle + \langle\mathcal{F}_d^2\rangle + \langle\mathcal{F}_e^2\rangle = 0, \quad \text{(C5)}$$

$$6\langle\mathcal{F}_Q^3\rangle + 2\langle\mathcal{F}_L^3\rangle - 3\langle\mathcal{F}_u^3\rangle - 3\langle\mathcal{F}_d^3\rangle - \langle\mathcal{F}_e^3\rangle - \langle\mathcal{F}_\nu^3\rangle = 0. \quad \text{(C6)}$$

In addition, avoiding $Z' - Z$ kinetic mixing at one loop requires [10,44]

$$\langle\mathcal{F}_Q\rangle - \langle\mathcal{F}_L\rangle + 2\langle\mathcal{F}_u\rangle - \langle\mathcal{F}_d\rangle - \langle\mathcal{F}_e\rangle = 0. \quad \text{(C7)}$$

Here, we use the notation $\langle X\rangle = \text{Tr}(X)$ and $\mathcal{F}_A = \text{diag}(F_{A_1}, F_{A_2}, F_{A_3})$ with $A = Q, u, d, L, e, \nu$. First, we focus on those equations that are linear with trace charge matrices, which are Eqs. (C1)–(C4) and (C7). Solving them, we find

$$\langle\mathcal{F}_Q\rangle = -\langle\mathcal{F}_u\rangle = \frac{1}{3}\langle\mathcal{F}_d\rangle = -\frac{1}{3}\langle\mathcal{F}_L\rangle = -\langle\mathcal{F}_e\rangle = -\frac{1}{5}\langle\mathcal{F}_\nu\rangle.$$

Setting $F_{Q_{1,2,3}} = 0$, we avoid kaon constraints and for the BMs III and IV couplings to the top, and arrive at the simple condition

$$\langle\mathcal{F}_Q\rangle = 0, \quad \text{(C8)}$$

and therefore from Eq. (C8) to

$$\langle \mathcal{F}_u \rangle = \langle \mathcal{F}_d \rangle = \langle \mathcal{F}_L \rangle = \langle \mathcal{F}_e \rangle = \langle \mathcal{F}_\nu \rangle = 0. \quad \text{(C9)}$$

Let us work on the remaining ACCs, Eqs. (C5) and (C6). The nonlinear behavior of these equations makes it challenging to solve them. We have already some information about the trace of these matrices; they are zero (C9). To solve the problem, mathematical relations between $\langle \mathcal{F}_A \rangle$, $\langle \mathcal{F}_A^2 \rangle$, and $\langle \mathcal{F}_A^3 \rangle$ would be helpful. Noting that for 3×3 matrices holds

$$\langle \mathcal{F}_A^3 \rangle - \frac{3}{2} \langle \mathcal{F}_A^2 \rangle \langle \mathcal{F}_A \rangle + \frac{1}{2} \langle \mathcal{F}_A \rangle^3 = 3 \det(\mathcal{F}_A), \quad \text{(C10)}$$

and $\det(\mathcal{F}_A) = F_{A_1} F_{A_2} F_{A_3}$, it follows from $\langle \mathcal{F}_A \rangle = 0$ that $\langle \mathcal{F}_A^3 \rangle$ vanishes if one charge vanishes, for instance, $F_{A_3} = 0$; then Eq. (C6) is fulfilled. In general, the charge matrices $\mathcal{F}_A$ can then be written as

$$\mathcal{F}_A = F_A \begin{pmatrix} +1 & 0 & 0 \\ 0 & -1 & 0 \\ 0 & 0 & 0 \end{pmatrix}, \qquad A = u, d, L, e, \nu, \quad \text{(C11)}$$

where F_A are integers. Note that the order of $(+1, -1, 0)$ can be changed for each species A independently. It remains to solve Eq. (C5), which now simply reduces to

$$F_d^2 + F_e^2 = F_L^2 + 2F_u^2. \quad \text{(C12)}$$

We can start exploring this equation by setting $F_e = F_L$. This solution is motivated from the phenomenological point of view because we need small values of lepton charges as well as being disconnected from quark charges. However, in this case, the system has only the trivial solution $F_u = F_d = 0$ because $F_d^2 = 2F_u^2$ can not be fulfilled for integers. Let us simplify (C12) by setting $F_L = 0$, which is motivated by the strong constraints on lepton couplings. We obtain

$$F_d^2 + F_e^2 = 2F_u^2. \quad \text{(C13)}$$

Two aspects are worth noting from this equation:

(a) For any Pythagorean triple (m, n, p), i.e., integers that solve the Pythagoras equation $m^2 + n^2 = p^2$, one can find integer triples (F_d, F_e, F_u), which solve Eq. (C13) by substituting $F_d = m + n$, $F_e = m - n$, and $F_u = p$.

(b) Any solution (F_d, F_e, F_u) to Eq. (C13) can be parametrized by integers (p, q, r),

$$F_d = p^2 + (-4r + 2q)p + 2r^2 - q^2, \quad \text{(C14)}$$

$$F_e = p^2 - 2r^2 - q^2 - 2pq + 4qr, \quad \text{(C15)}$$

$$F_u = p^2 + 2r^2 + q^2 - 2pr - 2qr. \quad \text{(C16)}$$

The first nontrivial solutions (F_d, F_e, F_u) are found to be

$$(F_d, F_e, F_u) = (1, 1, 1), (7, 1, 5), (17, 7, 13), \ldots, \quad \text{(C17)}$$

and so on, and integer multiples thereof. Note that each term can also have either sign, and that permutations between F_d and F_e are permitted.

Although Eq. (C13) gets fully solved by Eqs. (C14)–(C16), in the following, we illustrate a more practical approach that allows us to run directly into those solutions that accommodate the constraint given by Eq. (34). Let us rewrite (C13) as

$$\langle F | \mathcal{J} | F \rangle = F_e^2, \quad \text{(C18)}$$

with $|F\rangle = (F_u, F_d)$ and

$$\mathcal{J} = \begin{pmatrix} 2 & 0 \\ 0 & -1 \end{pmatrix}. \quad \text{(C19)}$$

For illustration, we start with the trivial solution $(F_d, F_e, F_u) = (1, 1, 1)$. Using Eq. (C18), we obtain

$$\langle F_0 | \mathcal{J} | F_0 \rangle = 1, \quad \text{(C20)}$$

with

$$|F_0\rangle = (1, 1). \quad \text{(C21)}$$

Now, the question we should ask is whether there are more solutions, such as $F_e \ll F_u, F_d$. One possibility is if a transformation

$$\mathcal{J} \to \mathcal{J}' = U^T \mathcal{J} U = \mathcal{J}, \quad \text{(C22)}$$

by a 2×2 matrix with integer entries U, leads invariant Eq. (C20) so that we can generate recursively solutions,

$$|F_i\rangle = (U)^i |F_0\rangle, \quad \text{(C23)}$$

which could get enlarged while keeping F_e fixed to 1 for this particular case. This matrix needs to satisfy

$$\begin{pmatrix} U_{11} & U_{12} \\ U_{21} & U_{22} \end{pmatrix}^T \begin{pmatrix} 2 & 0 \\ 0 & -1 \end{pmatrix} \begin{pmatrix} U_{11} & U_{12} \\ U_{21} & U_{22} \end{pmatrix} = \begin{pmatrix} 2 & 0 \\ 0 & -1 \end{pmatrix}. \quad \text{(C24)}$$

The solution of this system in terms of U_{22} is

$$U_{11} = \eta_{11} U_{22}, \tag{C25}$$

$$U_{12} = \eta_{12}\sqrt{\frac{-1+U_{22}^2}{2}}, \tag{C26}$$

$$U_{21} = \eta_{21}\sqrt{2(-1+U_{22}^2)}, \tag{C27}$$

with four solutions $(\eta_{11},\eta_{12},\eta_{22}) = (-1,-1,+1)$, $(-1,+1,-1)$, $(+1,-1,-1)$, and $(+1,+1,+1)$. The smallest integer solution reads

$$U = \begin{pmatrix} \eta_{11}3 & \eta_{12}2 \\ \eta_{21}4 & \eta_{22}3 \end{pmatrix}. \tag{C28}$$

We then find the solutions (C23) for any integer $i > 0$. Using $\eta_{12} = \eta_{22} = \eta_{11} = \eta_{21} = +1$ leads to

$$\begin{aligned} |F_1\rangle &= (5,7), \\ |F_2\rangle &= (29,41), \\ |F_3\rangle &= (169,239), \\ |F_4\rangle &= (985,1393), \\ |F_5\rangle &= (5741,8119), \\ &\vdots \end{aligned} \tag{C29}$$

We learn that, in order to avoid electron and muon constraints of Eq. (34), we need solutions $|F_i\rangle$ with $i \geq 4$. Note that we could have also used a different setup for $\eta_{11},\ldots$ to get different solutions. In addition, we can also find more solutions by choosing another initial integer triple (F_d, F_u, F_e).

In the phenomenological analysis, we considered the solution $i = 4$ for BM IV,

$$(F_d, F_e, F_u) = (1393, 1, 985), \tag{C30}$$

with zero neutrino charges $F_\nu = 0$.

APPENDIX D: KINETIC MIXING

In this appendix, we discuss the naturalness of the gauge-kinetic mixing, occurring due to the parameter η as in (35) between the Z' and the photon or, equivalently, the Z' and hypercharge gauge boson before electroweak symmetry breaking. Ideally, one would like the RG evolution of this parameter to be technically natural, which means

$$\frac{\mathrm{d}\eta}{\mathrm{d}\ln\mu} \propto \eta. \tag{D1}$$

This would imply that kinetic mixing can naturally be switched off at all scales or made to remain arbitrarily small.

For theories with the charge configuration (C11), as well as the Higgs not carrying a $U(1)'$ charge, kinetic mixing is natural at one-loop order. If only gauge contributions are taken into account, the naturalness remains intact even at higher loops, which is the result of the symmetry implied by (C11). We have verified that this is the case until four loops, using the results of [37,38].

Starting at two-loop order, Yukawa interactions violate the naturalness (D1), unless they retain certain flavor textures. If the top quark does not carry $U(1)'$ charge as in BM IV, the naturalness-violating terms do not feature the top Yukawa coupling at two loops and are either suppressed by the other much smaller Yukawas and/or loop factors. Thus, these terms are negligible for the running of η, which becomes effectively natural.

However, the naturalness is broken at one loop below the scale where the first field carrying $U(1)'$ charge is integrated out, i.e., the bottom quark in BM IV.

[1] LHCb Collaboration, Report No. CERN-EP-2022-163, LHCb-PAPER-2022-024, arXiv:2209.03179.
[2] R. Aaij *et al.* (LHCb Collaboration), Phys. Rev. Lett. **122**, 211803 (2019).
[3] S. Schacht, J. High Energy Phys. 03 (2023) 205.
[4] M. J. Savage, Phys. Lett. B **257**, 414 (1991).
[5] D. Pirtskhalava and P. Uttayarat, Phys. Lett. B **712**, 81 (2012).
[6] J. Brod, Y. Grossman, A. L. Kagan, and J. Zupan, J. High Energy Phys. 10 (2012) 161.
[7] G. Hiller, M. Jung, and S. Schacht, Phys. Rev. D **87**, 014024 (2013).
[8] T. Feldmann, S. Nandi, and A. Soni, J. High Energy Phys. 06 (2012) 007.
[9] Y. Amhis *et al.* (HFLAV Collaboration), Phys. Rev. D **107**, 052008 (2023).
[10] R. Bause, H. Gisbert, M. Golz, and G. Hiller, Phys. Rev. D **101**, 115006 (2020).
[11] Y. Grossman, A. L. Kagan, and Y. Nir, Phys. Rev. D **75**, 036008 (2007).
[12] J. Brod, A. L. Kagan, and J. Zupan, Phys. Rev. D **86**, 014023 (2012).
[13] W. Altmannshofer, R. Primulando, C. T. Yu, and F. Yu, J. High Energy Phys. 04 (2012) 049.

[14] R. Aaij *et al.* (LHCb Collaboration), Phys. Rev. Lett. **127**, 111801 (2021).
[15] LHCb Collaboration, Rare charm decays at LHCb, Marianna Fontana, in *Talk at ICHEP* (ICHEP 2022 Conference, Bologna, 2022).
[16] H. Gisbert, M. Golz, and D. S. Mitzel, Mod. Phys. Lett. A **36**, 2130002 (2021).
[17] J. Fuentes-Martin, A. Greljo, J. Martin Camalich, and J. D. Ruiz-Alvarez, J. High Energy Phys. 11 (2020) 080.
[18] M. Ablikim *et al.* (BESIII Collaboration), Phys. Rev. D **105**, L071102 (2022).
[19] R. Bause, H. Gisbert, M. Golz, and G. Hiller, Phys. Rev. D **103**, 015033 (2021).
[20] R. Bause, H. Gisbert, M. Golz, and G. Hiller, Eur. Phys. J. C **82**, 164 (2022).
[21] Y. T. Lai *et al.* (Belle Collaboration), Phys. Rev. D **95**, 011102 (2017).
[22] D. Wang, Eur. Phys. J. C **83**, 279 (2023).
[23] P. Ilten, Y. Soreq, M. Williams, and W. Xue, J. High Energy Phys. 06 (2018) 004.
[24] A. M. Sirunyan *et al.* (CMS Collaboration), Phys. Rev. Lett. **123**, 231803 (2019).
[25] B. A. Dobrescu and F. Yu, arXiv:2112.05392.
[26] B. A. Dobrescu and C. Frugiuele, Phys. Rev. Lett. **113**, 061801 (2014).
[27] A. Aranda and C. D. Carone, Phys. Lett. B **443**, 352 (1998).
[28] B. Batell, J. L. Feng, M. Fieg, A. Ismail, F. Kling, R. M. Abraham, and S. Trojanowski, Phys. Rev. D **105**, 075001 (2022).
[29] D. C. Bailey and S. Davidson, Phys. Lett. B **348**, 185 (1995).
[30] S. Cheng, A. Khodjamirian, and A. V. Rusov, Phys. Rev. D **102**, 074022 (2020).
[31] R. L. Workman *et al.* (Particle Data Group), Prog. Theor. Exp. Phys. **2022**, 083C01 (2022).
[32] C. Bruch, A. Khodjamirian, and J. H. Kuhn, Eur. Phys. J. C **39**, 41 (2005).
[33] R. Baldini Ferroli, A. Mangoni, and S. Pacetti, Phys. Rev. C **98**, 045210 (2018).
[34] M. Fabbrichesi, E. Gabrielli, and G. Lanfranchi, *The Physics of the Dark Photon* (Springer, Cham, 2021).
[35] R. Bause, G. Hiller, T. Höhne, D. F. Litim, and T. Steudtner, Eur. Phys. J. C **82**, 42 (2022).
[36] R. Aaij *et al.* (LHCb Collaboration), Phys. Rev. Lett. **124**, 041801 (2020).
[37] A. Bednyakov and A. Pikelner, Phys. Rev. Lett. **127**, 041801 (2021).
[38] J. Davies, F. Herren, and A. E. Thomsen, J. High Energy Phys. 01 (2022) 051.
[39] M. Campajola *et al.* (Belle II Collaboration), Phys. Scr. **96**, 084005 (2021).
[40] M. Ablikim *et al.* (BESIII Collaboration), Phys. Lett. B **839**, 137785 (2023).
[41] J. P. Lees *et al.* (*BABAR* Collaboration), Phys. Rev. Lett. **119**, 131804 (2017).
[42] R. Bause, M. Golz, G. Hiller, and A. Tayduganov, Eur. Phys. J. C **80**, 65 (2020); **81**, 219(E) (2021).
[43] B. C. Allanach, J. Davighi, and S. Melville, J. High Energy Phys. 02 (2019) 082; 08 (2019) 64(E).
[44] B. Holdom, Phys. Lett. **166B**, 196 (1986).